Journal of Solid State Chemistry **154,** 507–513 (2000)
doi:10.1006/jssc.2000.8871, available online at http://www.idealibrary.com on IDEAL®

A Three-Dimensional Iron(III) Phosphate, $[C_2N_2H_{10}]_2[Fe_5F_4(PO_4)(HPO_4)_6]$

Amitava Choudhury*,† and Srinivasan Natarajan*,[1]

*Chemistry and Physics of Materials Unit, Jawaharlal Nehru Centre for Advanced Scientific Research, Jakkur P.O., Bangalore 560 064, India; and †Solid State and Structural Chemistry Unit, Indian Institute of Science, Bangalore 560 012, India

Received April 25, 2000; in revised form June 26, 2000; accepted July 13, 2000; published online September 30, 2000

A new iron phosphate, $[C_2N_2H_{10}]_2[Fe_5F_4(PO_4)(HPO_4)_6]$, containing F^- ions as part of the framework, has been synthesized hydrothermally using iron acetylacetonate as the source for iron and ethylenediamine (*en*) as the amine. A network of $[Fe(O/F)_6]$ octahedra and PO_4 tetrahedra, linked through their vertices, forms the three-dimensional architecture with one-dimensional channels bound by 8-*T* atom (*T* = Fe, P), wherein the disordered *en* molecules are located. The connectivity between the Fe centers via Fe–O/F–Fe linkage giving rise to a pentamer unit is worthy of note. Crystal data: tetragonal, space group = $P4_32_12$, $a = 9.864(1)$, $c = 30.353(1)$ Å, $V = 2953.1(1)$ Å^3, $Z = 4$, $R_1 = 0.025$, w$R_2 = 0.066$. © 2000 Academic Press

INTRODUCTION

A large number of metal phosphates with open architectures have been synthesized in recent years (1). Of these, those of the transition elements are particularly fascinating due to the possibility of the variations in coordination environments around the metal ion as well as the possibility of observing interesting magnetic behavior. Thus, several open-framework iron phosphates have been synthesized and characterized recently (2–18). The iron phosphate structures, generally, comprise a vertex linkage between the Fe–O polyhedra and the PO_4 tetrahedra, forming chain, layer, and three-dimensional structures. The open-framework iron phosphates are sometimes synthesized hydrothermally employing F^- ions, which often get incorporated as part of the framework and act as a bridge between the Fe centers. In this connection, the recent report of a novel three-dimensional iron phosphate, synthesized by us, possessing infinite Fe–O/F–Fe linear one-dimensional chains, exhibiting a gradual spin-crossover behavior from the low- to the high-spin state as a function of temperature is noteworthy (18). Our continued efforts on the synthesis of iron phosphates enabled us to discover a new three-dimensional iron(III) phosphate, $[C_2N_2H_{10}]_2[Fe_5F_4(PO_4)(HPO_4)_6]$, possessing channels bound by 8-*T* atoms (*T* = Fe, P), wherein the amine molecule (*en*, $H_3N(CH_2)_2NH_3$) is located in the channels.

[1] To whom correspondence should be addressed. Fax: + (80)-846-2766. E-mail: raj@jncasr.ac.in.

EXPERIMENTAL

The title compound was synthesized from a gel containing ethylenediamine (*en*) as the amine. In a typical synthesis, 0.529 g of iron acetylacetonate $[Fe(acac)_3]$ dispersed in 2.7 ml of water with constant stirring. To this, 0.1 ml of *en* was slowly added followed by the addition of 0.2 ml of phosphoric acid (aq. 85 wt%). Finally, 0.05 ml of HF (48%) was added and the mixture was stirred until homogeneous. The final mixture, with the composition $Fe(acac)_3 : 2H_3PO_4 : en : 3HF : 100H_2O$, was transferred into a 7-ml PTFE-lined acid digestion bomb and heated at 453 K for 72 h. The fill factor was ~50%. The resultant product contained only colorless truncated octahedral-shaped crystals, suitable for single crystal X-ray diffraction and was filtered and washed thoroughly with deionized distilled water. The initial characterization was carried out using powder X-ray diffraction (XRD) and thermogravimetric analysis (TGA). The powder XRD pattern indicated that the product is a new material; the pattern is entirely consistent with the structure determined by single-crystal X-ray diffraction. The unit-cell parameters generated by the least-squares fit of the powder XRD (Cu$K\alpha$) lines, using the *hkl* indices generated from single-crystal XRD data, was in good agreement with that determined using the single-crystal XRD. Powder data for the iron phosphate, $[C_2N_2H_{10}]_2[Fe_5F_4(PO_4)(HPO_4)_6]$, are listed in Table 1. EDAX analysis indicated that the ratio between Fe and P is 5 : 7, consistent with the stoichiometry determined by single crystal studies. Fluorine content was determined using quantitative chemical analysis, which indicates the presence of 6.1 w% of fluorine (calc. = 6.6%), in agreement with the chemical formula of the compound.

A suitable colorless single crystal of the title compound was carefully selected under a polarizing microscope and glued to a thin glass fiber with cyanoacrylate (superglue)

0022-4596/00 $35.00

TABLE 1
X-ray Powder Data for $[C_2N_2H_{10}]_2[Fe_5(PO_4)(HPO_4)_6F_4]$

h	k	l	$2\theta_{obs}$	$\Delta(2\theta)^a$	D_{calc}	d_{obs}	$\Delta(d)^b$	I^c_{rel}
1	0	1	9.497	0.013	9.325	9.312	− 0.013	9.74
1	0	2	10.749	− 0.011	8.222	8.230	0.008	9.67
0	0	4	11.730	0.002	7.546	7.544	− 0.002	36.83
1	1	0	12.784	0.016	6.933	6.924	− 0.009	26.20
1	1	2	14.073	0.015	6.300	6.293	− 0.007	10.93
1	1	3	15.515	− 0.007	5.709	5.711	0.002	100.00
2	0	2	19.019	− 0.015	4.662	4.666	0.004	4.48
2	1	1	20.463	− 0.004	4.339	4.340	0.001	8.20
2	1	3	22.122	0.008	4.020	4.018	− 0.002	6.64
0	0	8	23.579	− 0.002	3.773	3.773	0.000	6.81
1	1	7	24.304	− 0.004	3.661	3.662	0.001	22.51
0	1	8	25.308	0.015	3.521	3.519	− 0.002	2.00
2	2	3	27.203	− 0.006	3.277	3.278	0.001	14.07
3	0	2	27.924	− 0.008	3.194	3.195	0.001	14.13
2	2	4	28.331	− 0.001	3.150	3.150	0.000	17.65
3	1	1	28.950	0.002	3.084	3.084	0.000	11.88
3	1	2	29.408	0.000	3.037	3.037	0.000	10.62
2	0	9	32.333	− 0.010	2.768	2.769	0.001	3.14
2	2	7	33.142	− 0.017	2.702	2.703	0.001	17.53
1	0	11	33.932	0.007	2.642	2.642	0.000	1.00
4	1	5	40.791	0.008	2.212	2.212	0.000	3.08
2	2	11	41.989	− 0.004	2.151	2.152	0.001	2.82
3	3	7	44.489	0.011	2.037	2.036	− 0.001	7.29

Note. Refined lattice parameter from powder data (Cu$K\alpha$): $a = 9.804(1)$, $c = 30.182(4)$ Å.
[a] $2\theta_{obs} - 2\theta_{calc}$.
[b] $d_{obs} - d_{calc}$.
[c] $100 \times I/I_{max}$.

adhesive. Crystal structure determination by X-ray diffraction was performed on a Siemen's SMART-CCD diffractometer equipped with a normal focus, 2.4-kW sealed-tube X-ray source (Mo$K\alpha$ radiation, $\lambda = 0.71073$ Å) operating at 50 kV and 40 mA. A hemisphere of intensity data were collected at room temperature in 1321 frames with ω scans (width of 0.30° and exposure time of 10 s per frame) in the 2θ range 3 to 46.5°. Pertinent experimental details for the structure determinations are presented in Table 2. An absorption correction based on symmetry equivalent reflections was applied using SADABS (19) program. Other effects, such as absorption by the glass fiber, were simultaneously corrected. The reduced data indicated $P4_32_12$ and $P4_12_12$ as the likely space groups. The initial structure was solved by direct methods using SHELXS-86 (20) in the space group $P4_32_12$, which readily established the heavy atom (Fe, P) sites and most of the light atom (O, N, F, and C) positions. One of the nitrogen atoms of the amine molecule [N(2)] was found to be disordered with a total SOF of 0.61(3) and 0.38(6), respectively. All the hydrogen positions were located from difference Fourier maps and for the final refinement the hydrogens were placed geometrically and held in the riding mode. The structural refinement converged to a $R_1 = 0.025$, $wR_2 = 0.066$, and the absolute structure parameter (21) (Flack parameter, x) to 0.00(2), indicating the correctness of the space group. Since the reduced data indicated two different space groups, we proceeded to solve the structure in $P4_12_12$. Again a very good initial model was established by direct methods and the refinement converged to a $R_1 = 0.025$, $wR_2 = 0.071$, and the Flack parameter $x = 0.02(2)$. Inverting the structural solution in both the cases results in the Flack parameter x being greater than 0. Typically, $x = 0.87$ in both the cases. Possibly, the crystals were twinned racemically. The relevant details of the structure determination in the $P4_32_12$ space group are presented in Table 2. Full-matrix least-squares refinement on $|F^2|$ (atomic coordinates, anisotropic thermal parameters for the nonhydrogen atoms of the framework, water, and amine molecule) were carried out using the program SHELXTL-PLUS (22). The final atomic coordinates along with the thermal parameters for $[C_2N_2H_{10}]_2[Fe_5F_4(PO_4)(HPO_4)_6]$ is presented in Table 3 and the bond distances and angles in Table 4 and 5.

RESULTS AND DISCUSSION

Iron-phosphate, $[C_2N_2H_{10}]_2[Fe_5F_4(PO_4)(HPO_4)_6]$, is a new three-dimensional open-framework structure made

TABLE 2
Crystal Data and Structural Refinement Parameters for $[C_2N_2H_{10}]_2[Fe_5(PO_4)(HPO_4)_6F_4]$

Empirical formula	$Fe_5P_7O_{28}F_4C_4N_4H_{26}$
Crystal system	Tetragonal
Space group	$P4_32_12$
T(K)	293(2)
Crystal Size (mm)	$0.08 \times 0.16 \times 0.20$
a (Å)	9.8636(1)
c (Å)	30.3529(6)
Volume (Å^3)	2953.1(1)
Z	4
Formula mass	1150.28
ρ_{calc} (g cm^{-3})	2.582
λ (Mo$K\alpha$) Å	0.71073
μ (mm^{-1})	2.922
θ Range (°)	1.34–23.20
Total data collected	12384
Index ranges	$-7 \le h \le 10, -10 \le k \le 10, -33 \le l \le 29$
Unique data	2105
Observed data ($\sigma > 2\sigma$(I))	2006
Refinement method	Full-matrix least-squares on $\|F^2\|$
R indices [$I > 2\sigma(I)$]	$R_1 = 0.025$, $wR_2 = 0.066$
R indices (all data)	$R_1 = 0.029$, $wR_2 = 0.068^a$
Goodness of fit (S)	1.11
No. of variables	247
Largest difference map peak and hole eÅ^{-3}	0.615 and − 0.585

[a] $W = 1/[\sigma^2(F_O)^2 + (0.0322P)^2 + 3.283P]$, where $P = [F_O^2 + 2F_C^2]/3$.

TABLE 3
Atomic Coordinates (× 10⁴) and Equivalent Isotropic Displacement Parameters (Å² × 10³) for $[C_2N_2H_{10}]_2[Fe_5(PO_4)(HPO_4)_6F_4]$

Atom	*x*	*Y*	*z*	*U*(eq)[a]
Fe(1)	2297(1)	4206(1)	908(1)	8(1)
Fe(2)	− 499(1)	4072(1)	113(1)	9(1)
Fe(3)[b]	6888(1)	6888(1)	0	9(1)
P(1)	− 556(1)	2781(1)	1098(1)	10(1)
P(2)[b]	2370(1)	2370(1)	0	9(1)
P(3)	1758(1)	5298(1)	1943(1)	12(1)
P(4)	3782(1)	6552(1)	306(1)	11(1)
O(1)	2942(3)	3144(3)	398(1)	15(1)
O(2)	3108(3)	5935(3)	707(1)	14(1)
O(3)	3923(3)	3574(3)	1228(1)	12(1)
O(4)	1714(3)	5221(3)	1445(1)	15(1)
O(5)	997(3)	2716(3)	1080(1)	12(1)
F(6)	731(3)	4929(3)	535(1)	15(1)
O(7)	− 1975(3)	3310(3)	− 240(1)	14(1)
O(8)	8(3)	5334(3)	− 373(1)	16(1)
O(9)	825(3)	2636(3)	− 47(1)	15(1)
O(10)	− 1222(3)	3074(3)	646(1)	13(1)
F(11)	− 1830(3)	5650(3)	323(1)	13(1)
O(12)	7363(3)	8352(3)	407(1)	17(1)
O(13)	5318(3)	6446(3)	369(1)	16(1)
O(14)	− 1046(3)	3983(3)	1398(1)	16(1)
O(15)	2789(4)	4240(4)	2141(1)	25(1)
O(16)	3345(3)	5798(3)	− 132(1)	20(1)
N(1)	6513(4)	4968(4)	1052(1)	20(1)
C(1)	6671(6)	6137(7)	1355(2)	39(2)
C(2)	5416(8)	6454(9)	1604(3)	65(2)
N(2)[c]	5329(9)	7302(9)	1910(3)	40(3)
N(2A)[c]	5393(14)	5727(15)	2016(5)	49(5)

[a] *U*(eq) is defined as one third of the trace of the orthogonalized U_{ij} tensor.
[b] Site occupancy factor SOF = 0.5.
[c] Refined SOF[*N*(2)] = 0.61(3); SOF[*N*(2A)] = 0.38(6).

from the linkages involving FeO_6 octahedra and PO_4 tetrahedra incorporating the diprotonated *en* molecules within its pores. The asymmetric unit of the iron phosphate consists of 27 nonhydrogen atoms, of which 23 belong to the "framework" and 4 to the "guest" as shown in Fig. 1. There are three crystallographically independent Fe and four P atoms, of which one iron and phosphorus atom [Fe(3), P(2)] sits in a special position with occupancy of 0.5.

The Fe atoms are octahedrally coordinated with respect to their oxygen/fluorine neighbors with Fe–O/F distances in the range 1.957(3)–2.134(3) Å (av. Fe(1)–O/F = 1.998, Fe(2)–O/F = 2.009, Fe(3)–O/F = 1.977 Å); the longer distances mostly correspond to the Fe–F linkages (Table 4). Of the three Fe atoms, Fe(1) makes five Fe–O–P bonds and one Fe–F–Fe bond, Fe(2) and Fe(3) makes four Fe–O–P bonds and two Fe–F–Fe linkages. The Fe–O–P bonds have an average bond angle of 136.7° and an angle of 133.2° for the Fe–F–Fe linkage. The fluorine atoms act as a bridge between the Fe centers, similar to the many phosphates of iron reported in the literature (2–18). These geometrical data are in good agreement with the results of previous structure determinations on similar compounds. Of the four distinct P atoms, three P atoms make three P–O–Fe bonds and possess one terminal P–O linkage and one P atom makes four P–O–Fe bonds. The P–O bond distances are in the range 1.514(3)–1.582(3) Å (av. P(1)–O = 1.546, P(2)–O = 1.544, P(3)–O = 1.540, P(4)–O = 1.542 Å) and O–P–O angles are in the range 102.0–113.7°. A framework structure of $Fe_{2.5}F_2(PO_4)_{3.5}$ would give a net framework charge of − 5. The presence of $[C_2N_2H_{10}]$ would account for + 2 charge arising from the complete protonation of the amine. The excess negative charge of − 3 is then balanced by the protonation of the PO_4 moieties as given in the formula. Bond valence sum calculations (23) indicate that P(1)–O(14), P(3)–O(15), and P(4)–O(16) with distances of 1.571(3), 1.576(4), 1.582(3) Å, respectively, are formally –OH groups, which is also consistent with the proton positions observed in the difference Fourier maps. Similar P–OH bond lengths have been observed before (2–18).

The complex structure of the title compound can be understood by considering simpler secondary building units (SBUs). Thus, the polyhedral connectivity between the $Fe(O/F)_6$ octahedra and PO_4 tetrahedra forms a short-chain pentamer unit consisting of essentially Fe–F–Fe linkages as shown in Fig. 2a. The formation of short chain

TABLE 4
Selected Bond Distances in $[C_2N_2H_{10}]_2[Fe_5(PO_4)(HPO_4)_6F_4]$

Bond	Distance (Å)	Bond	Distance (Å)
Fe(1)–O(1)	1.975(3)	Fe(3)–F(11)[a]	2.013(2)
Fe(1)–O(2)	1.980(3)	P(1)–O(3)[b]	1.526(3)
Fe(1)–O(2)	1.975(3)	P(1)–O(5)	1.534(3)
Fe(1)–O(4)	1.996(3)	P(1)–O(10)	1.549(3)
Fe(1)–O(5)	2.018(3)	P(1)–O(14)	1.571(3)
Fe(1)–F(6)	2.044(3)	P(2)–O(1)[c]	1.537(3)
Fe(2)–O(7)	1.957(3)	P(2)–O(1)	1.537(3)
Fe(2)–F(6)	1.958(3)	P(2)–O(9)	1.553(3)
Fe(2)–O(9)	1.987(3)	P(2)–O(9)[c]	1.553(3)
Fe(2)–O(8)	1.992(3)	P(3)–O(4)	1.514(3)
Fe(2)–O(10)	2.023(3)	P(3)–O(12)[d]	1.529(4)
Fe(2)–F(11)	2.134(3)	P(3)–O(8)[e]	1.542(3)
Fe(3)–O(12)[c]	1.958(3)	P(3)–O(15)	1.576(4)
Fe(3)–O(12)	1.958(3)	P(4)–O(2)	1.515(3)
Fe(3)–O(13)	1.961(3)	P(4)–O(13)	1.531(3)
Fe(3)–O(13)[c]	1.961(3)	P(4)–O(7)[f]	1.539(3)
Fe(3)–F(11)[f]	2.013(2)	P(4)–O(16)	1.582(3)
		Organic moiety	
N(1)–C(1)	1.483(7)	C(2)–N(2)	1.252(10)
C(1)–C(2)	1.484(8)	C(2)–N(2A)	1.441(14)

Note. Symmetry transformations used to generate equivalent atoms: [a] $x + 1, y, z$. [b] $x - 1/2, -y + 1/2, -z + 1/4$. [c] $y, x, -z$. [d] $x - 1/2, -y + 3/2, -z + 1/4$. [e] $y - 1/2, -x + 1/2, z + 1/4$. [f] $y, x + 1, -z$.

TABLE 5
Selected Bond Angles in $[C_2N_2H_{10}]_2[Fe_5(PO_4)(HPO_4)_6F_4]$

Moiety	Angle (°)	Moiety	Angle (°)
O(1)–Fe(1)–O(3)	87.44(13)	O(12)–Fe(3)–F(11)[a]	89.43(12)
O(1)–Fe(1)–O(2)	94.87(13)	O(13)–Fe(3)–F(11)[a]	94.74(12)
O(3)–Fe(1)–O(2)	95.44(13)	O(13)[b]–Fe(3)–F(11)[a]	86.50(12)
O(1)–Fe(1)–O(4)	176.87(13)	F(11)[c]–Fe(3)–F(11)[a]	178.3(2)
O(3)–Fe(1)–O(4)	89.56(13)	O(3)[d]–P(1)–O(5)	108.2(2)
O(2)–Fe(1)–O(4)	86.32(13)	O(3)[d]–P(1)–O(10)	109.2(2)
O(1)–Fe(1)–O(5)	91.21(13)	O(5)–P(1)–O(10)	113.6(2)
O(3)–Fe(1)–O(5)	99.17(13)	O(3)[d]–P(1)–O(14)	110.8(2)
O(2)–Fe(1)–O(5)	164.41(13)	O(5)–P(1)–O(14)	111.1(2)
O(4)–Fe(1)–O(5)	88.37(13)	O(10)–P(1)–O(14)	104.0(2)
O(1)–Fe(1)–F(6)	89.65(12)	O(1)[b]–P(2)–O(1)	104.7(3)
O(3)–Fe(1)–F(6)	174.73(12)	O(1)[b]–P(2)–O(9)	110.7(2)
O(2)–Fe(1)–F(6)	80.44(12)	O(1)–P(2)–O(9)	110.4(2)
O(4)–Fe(1)–F(6)	93.41(12)	O(1)[b]–P(2)–O(9)[b]	110.4(2)
O(5)–Fe(1)–F(6)	85.27(12)	O(1)–P(2)–O(9)[b]	110.7(2)
O(7)–Fe(2)–F(6)	170.17(12)	O(9)–P(2)–O(9)[b]	109.9(3)
O(7)–Fe(2)–O(9)	94.68(13)	O(4)–P(3)–O(12)[e]	110.7(2)
F(6)–Fe(2)–O(9)	93.47(12)	O(4)–P(3)–O(8)[f]	109.1(2)
O(7)–Fe(2)–O(8)	91.29(14)	O(12)[e]–P(3)–O(8)[f]	114.7(2)
F(6)–Fe(2)–O(8)	93.36(12)	O(4)–P(3)–O(15)	111.5(2)
O(9)–Fe(2)–O(8)	95.75(13)	O(12)[e]–P(3)–O(15)	102.2(2)
O(7)–Fe(2)–O(10)	89.33(13)	O(8)[f]–P(3)–O(15)	108.6(2)
F(6)–Fe(2)–O(10)	84.54(12)	O(2)–P(4)–O(13)	107.8(2)
O(9)–Fe(2)–O(10)	94.61(14)	O(2)–P(4)–O(7)[c]	110.6(2)
O(8)–Fe(2)–O(10)	169.54(14)	O(13)–P(4)–O(7)[c]	112.4(2)
O(7)–Fe(2)–F(11)	89.21(12)	O(2)–P(4)–O(16)	111.5(2)
F(6)–Fe(2)–F(11)	82.54(10)	O(13)–P(4)–O(16)	110.0(2)
O(9)–Fe(2)–F(11)	175.91(11)	O(7)[c]–P(4)–O(16)	104.6(2)
O(8)–Fe(2)–F(11)	85.40(12)	P(2)–O(1)–Fe(1)	139.6(2)
O(10)–Fe(2)–F(11)	84.17(12)	P(4)–O(2)–Fe(1)	140.5(2)
O(12)[b]–Fe(3)–O(12)	92.6(2)	P(1)[g]–O(3)–Fe(1)	136.1(2)
O(12)[b]–Fe(3)–O(13)	175.37(14)	P(3)–O(4)–Fe(1)	146.2(2)
O(12)–Fe(3)–O(13)	89.54(14)	P(1)–O(5)–Fe(1)	127.8(2)
O(12)[b]–Fe(3)–O(13)[b]	89.54(14)	Fe(2)–F(6)–Fe(1)	132.89(13)
O(12)–Fe(3)–O(13)[b]	175.37(14)	P(4)[h]–O(7)–Fe(2)	131.1(2)
O(13)–Fe(3)–O(13[b]	88.6(2)	P(3)[i]–O(8)–Fe(2)	142.1(2)
O(12)[b]–Fe(3)–F(11)[c]	89.43(12)	P(2)–O(9)–Fe(2)	138.0(2)
O(12)–Fe(3)–F(11)[c]	89.38(12)	P(1)–O(10)–Fe(2)	130.5(2)
O(13)–Fe(3)–F(11)[c]	86.49(12)	Fe(3)[j]–F(11)–Fe(2)	133.10(12)
O(13)[b]–Fe(3)–F(11)[c]	94.74(12)	P(3)[k]–O(12)–Fe(3)	137.5(2)
O(12[b]–Fe(3)–F(11)[a]	89.38(12)	P(4)–O(13)–Fe(3)	134.0(2)
		Organic moiety	
N(1)–C(1)–C(2)	113.1(6)	N(2A)–C(2)–C(1)	110.5(9)
N(2)–C(2)–C(1)	125.2(8)		

Note. Symmetry transformations used to generate equivalent atoms: [a] $x+1, y, z$. [b] $y, x, -z$. [c] $y, x+1, -z$. [d] $x-1/2, -y+1/2, -z+1/4$. [e] $x-1/2, -y+3/2, -z+1/4$. [f] $y-1/2, -x+1/2, z+1/4$. [g] $x+1/2, -y+1/2, -z+1/4$. [h] $y-1, x, -z$. [i] $9-y+1/2, x+1/2, z-1/4$. [j] $x-1, y, z$. [k] $x+1/2, -y+3/2, -z+1/4$.

Fe–O/F–Fe linkages of the type observed in the present case, and/or infinite one-dimensional chains has been observed in many of the open-framework iron phosphates reported in the literature (5–7, 18). The phosphorus atom P(2) links these chains via P–O–Fe bonds, and the other phosphorus atoms are grafted onto these chains, completing the building unit of the iron phosphate. The building units are so arranged as to form a twofold screw axis along the *b* axis (Fig. 2b). The connectivity between these building units forms a layer with a 10-membered aperture, along *ab* direction, as shown in Fig. 3. The positions of individual layers are such that these apertures are inaccessible and do not form as channels along the *c* axis. This situation can be observed more clearly along the *a* axis, where the connectivity between the polyhedra are such that it appears as if alternate channels are accessible (Fig. 4). It is primarily due to the connectivity between the pentameric Fe–O/F–Fe units and the $P(1)O_4$ and $P(2)O_4$ moieties that the channels are rendered inaccessible. This type of connectivity is rather unusual and it is the first time such architecture has been observed in an open-framework phosphate of iron.

Thermogravimetric analysis of $[C_2N_2H_{10}]_2[Fe_5F_4(PO_4)(HPO_4)_6]$ was carried out in a N_2 atmosphere from room temperature to 800°C using a heating rate of 10°C min^{-1}, as shown in Fig. 5. The result shows two mass losses, a sharp one and a second rather broad one. The first mass loss of about 12.5%, occurring in the region 370–420°C, corresponds to the loss of the amine and some adsorbed water (calc. 11%) and the second mass loss of 8.2%, in the region 430–600°C, corresponds to the loss of the –OH group and fluorine (calc. 9.4%). The loss of the amine, the –OH group, and fluorine resulted in the collapse of the framework. The powder XRD pattern of the calcined material indicates the formation of a poorly crystalline material with all the XRD lines corresponding to the condensed iron phosphate, $FePO_4$ (JCPDS: 29-0715).

The variation of magnetic susceptibility as a function of temperature for $[C_2N_2H_{10}]_2[Fe_5F_4(PO_4)(HPO_4)_6]$ was carried out using a Lewis coil magnetometer. The results indicate a continuous variation of the susceptibility as a function of temperature, as shown in Fig. 6. The plot of inverse susceptibility vs temperature in the region of 300–150 K indicates a Curie–Weiss behavior with $\theta_p = -184.7$ and $\mu_{eff} = 6.25\ \mu B$. The μ_{eff} value is larger than the typical spin-only value for the high-spin Fe^{III} ($\mu_{spin-only} = 5.9\ \mu B$)[2f]. The larger negative value of θ_p suggests a predominantly anti-ferromagnetic interaction. The origin of anti-ferromagnetic interactions can be understood through the superexchange mechanism. In the structure, the strongest superexchange interactions may be originating from the Fe^{III}–O/F–Fe^{III} (high-spin, d^5–d^5 interaction) (24) present within the pentamer. These interactions are antiferromagnetically coupled via the phosphate units with the adjacent pentamer, giving rise to the observed behavior.

The synthesis of a phosphate of iron, $[C_2N_2H_{10}]_2[Fe_5(PO_4)(HPO_4)_6F_4]$, has been accomplished by the use of a novel precursor for iron. The importance and the role of the precursors in the synthesis and formation of framework solids have been emphasized time and again. Recently, it is

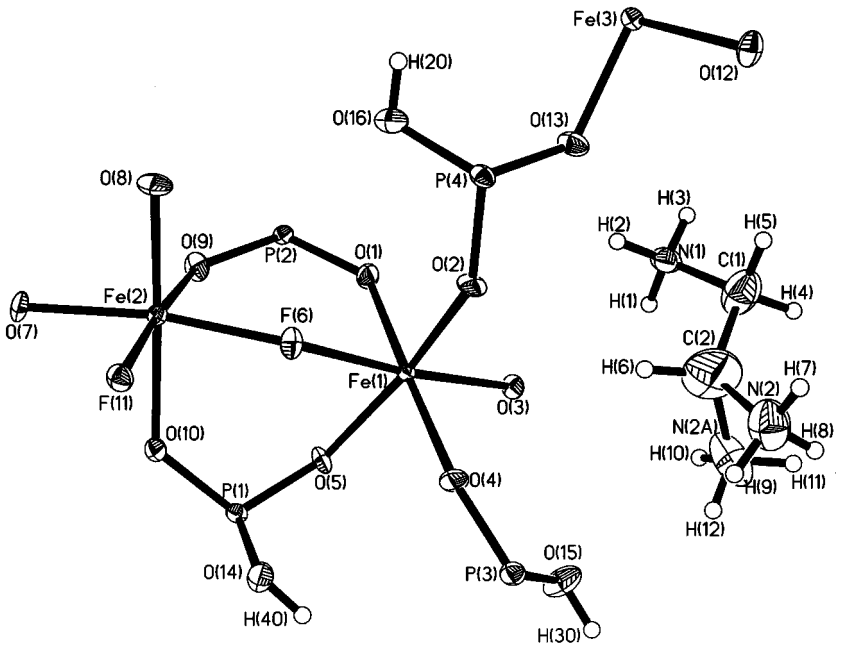

FIG. 1. ORTEP plot of the iron phosphate, $[C_2N_2H_{10}]_2[Fe_5F_4(PO_4)(HPO_4)_6]$. Thermal ellipsoids are given at 50% probability.

observed that the use of amine phosphates as starting materials leads to the formation of a variety of interesting framework architectures (25, 26). It is possible that the amine phosphate is not only the source for both the amine and phosphorus, but also acts as a complex template species *in situ*. The use of metal–amine complexes, on the

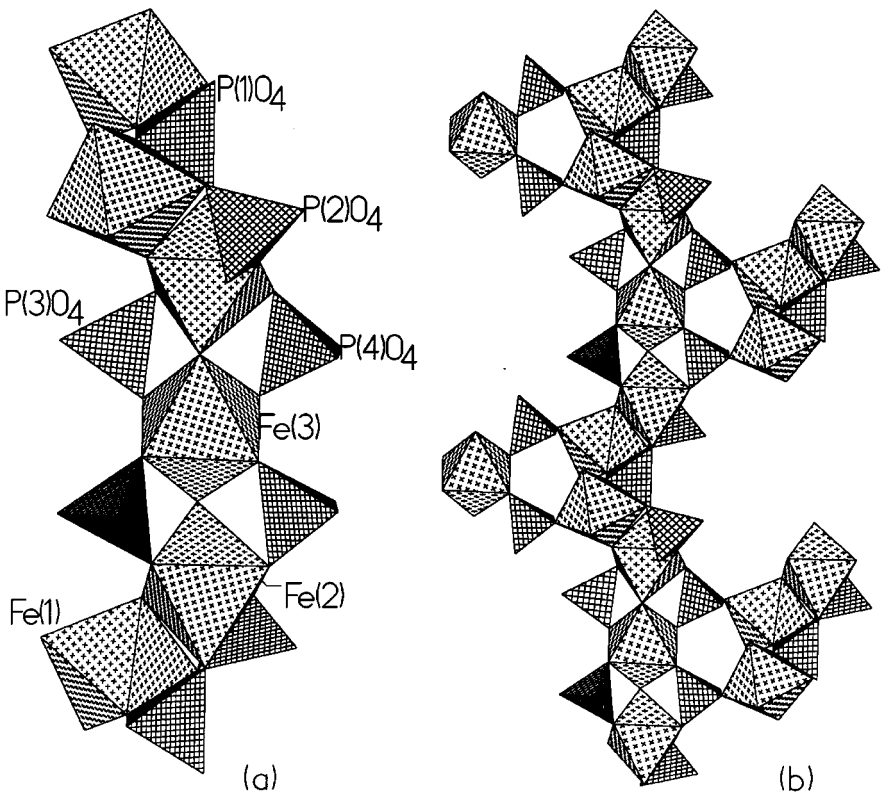

FIG. 2. (a) Figure showing the connectivity between the $Fe(O/F)_6$ octahedra and the PO_4 tetrahedra in $[C_2N_2H_{10}]_2[Fe_5F_4(PO_4)(HPO_4)_6]$. Note that the connectivity forms a pentamer linear chain of Fe–O/F–Fe. (b) Figure showing the two-fold screw axis present in the iron phosphate.

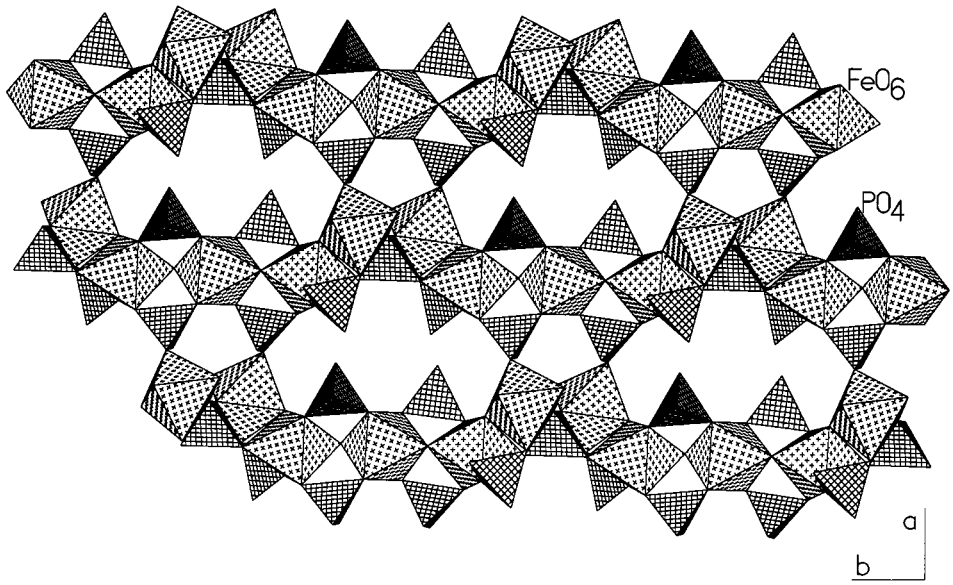

FIG. 3. Structure of the iron phosphate, $[C_2N_2H_{10}]_2[Fe_5F_4(PO_4)(HPO_4)_6]$, showing the connectivity between the polyhedra along the *c* axis.

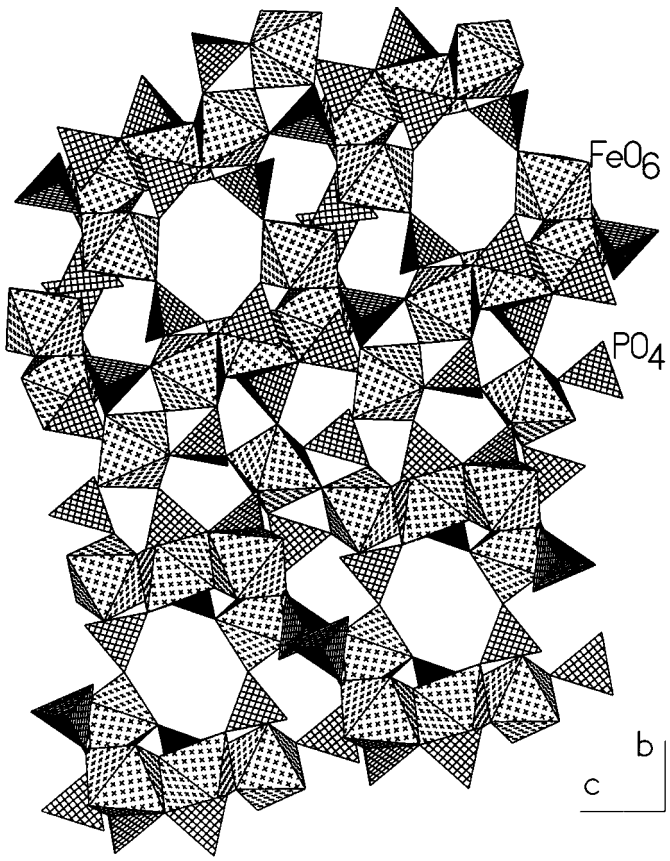

FIG. 4. Structure showing the one-dimensional channels along the *a* axis. The diprotonated amine molecules reside in these channels (not shown).

other hand, as possible precursors has been investigated in recent years, though not exhaustively, giving rise to novel structures (27). It is very likely, in these situations, that the release of the amine as well as the metal ion into solution is controlled by the careful variation of experimental parameters, during the synthesis. It is to be noted that previous use of ethylenediamine as the amine resulted in the formation of five different open-framework iron phosphate structures (2–10, 12, 13, 17), wherein the dimensionality changes from two to three depending on the synthetic conditions. In most of these syntheses, the starting source for iron is generally iron chloride, $FeCl_3 \cdot 6H_2O$. It is likely that the use of a new precursor for iron, may be partly responsible for formation of the new iron phosphate, $[C_2N_2H_{10}]_2$

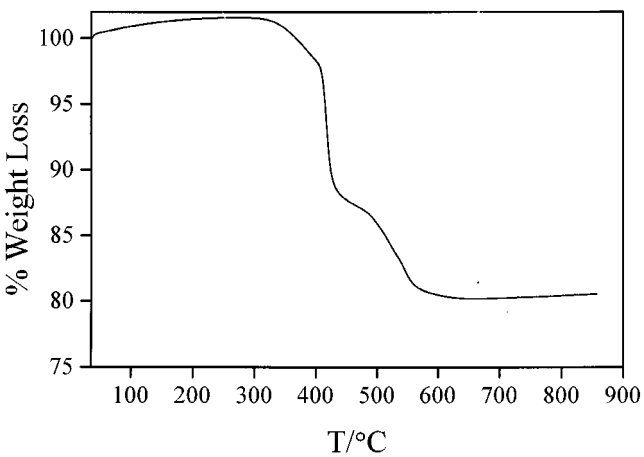

FIG. 5. TG curve of the iron phosphate, $[C_2N_2H_{10}]_2[Fe_5F_4(PO_4)(HPO_4)_6]$, showing the weight loss. Note the sharp weight loss in the region $\sim 400°C$.

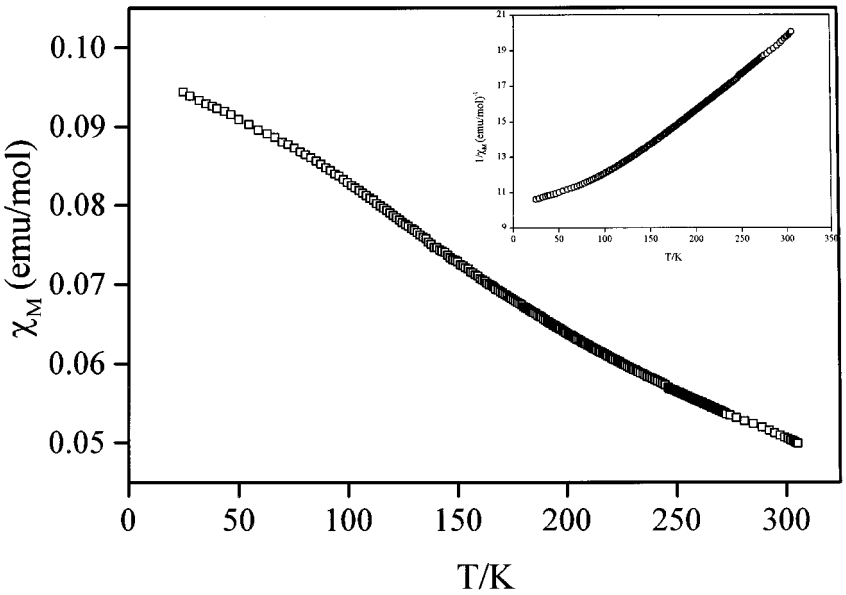

FIG. 6. Variation of magnetic susceptibility as a function of temperature for $[C_2N_2H_{10}]_2[Fe_5F_4(PO_4)(HPO_4)_6]$. (Inset) The inverse susceptibility vs temperature.

$[Fe_5F_4(PO_4)(HPO_4)_6]$. Work on the use of other precursors in the synthesis of open-framework iron phosphates is currently in progress.

ACKNOWLEDGMENTS

The authors thank Professor C. N. R. Rao, FRS, for his kind help, support, and encouragement. The authors also thank Professor A. R. Chakraborty, Inorganic and Physical Chemistry Departments, Indian Institute of Science, Bangalore, for magnetic susceptibility measurements. A.C. thanks the Council of Scientific and Industrial Research (CSIR), Government of India, for the award of a research fellowship.

REFERENCES

1. A. K. Cheetham, T. Loiseau, and G. Ferey, *Angew. Chem. Int. Ed.* **38,** 3268 (1999).
2. M. Cavellec, D. Riou, and G. Ferey, *J. Solid State Chem.* **112,** 441 (1994).
3. M. Cavellec, D. Riou, J.-M. Greneche, and G. Ferey, *Zeolites* **17,** 252 (1996).
4. M. Cavellec, C. Egger, J. Linares, M. Nogues, F. Varret, and G. Ferey, *J. Solid State Chem.* **134,** 349 (1997).
5. M. R. Cavellec, J.-M. Greneche, D. Riou, and G. Ferey, *Chem. Mater.* **10,** 2434 (1998).
6. M. Cavellec, J.-M. Greneche, D. Riou, and G. Ferey, *Microporous Mater.* **8,** 103 (1997).
7. M. Cavellec, D. Riou, J.-M. Greneche, and G. Ferey, *J. Magn. Magn. Mater.* **163,** 173 (1996).
8. M. Cavellec, D. Riou, and G. Ferey, *Acta Crystallogr.* **C51,** 2242 (1995).
9. M. Riou-Cavellec, J.-M. Greneche, and G. Ferey, *J. Solid State Chem.* **148,** 150 (1999).
10. C.-Y. Huang, S.-L. Wang, and K.-H. Lii, *J. Porous Mater.* **5,** 147 (1998).
11. K.-H. Lii, Y.-F. Huang, V. Zima, C.-Y. Huang, H.-M. Lin, Y.-C. Jiang, F.-L. Liao, and S.-L. Wang, *Chem. Mater.* **10,** 2599 (1998), and references therein.
12. J. R. D. DeBord, W. M. Reiff, C. J. Warren, R. C. Haushalter, and J. Zubieta, *Chem. Mater.* **9,** 1994 (1997).
13. J. R. D. DeBord, W. M. Reiff, R. C. Haushalter, and J. Zubieta, *J. Solid State Chem.* **125,** 186 (1996).
14. A. Mgaidi, H. Boughzala, A. Driss, R. Clerac, and C. Coulon, *J. Solid State Chem.* **144,** 163 (1999).
15. Z. A. D. Lethbridge, P. Lightfoot, R. E. Morris, D. S. Wragg, P. A. Wright, Å. Kvick, and G. Vaughan, *J. Solid State Chem.* **142,** 455 (1999).
16. A. Choudhury, and S. Natarajan, *Proc. Ind. Acad. Sci.* (*Chem. Sci.*) **111,** 627 (1999).
17. A. Choudhury, and S. Natarajan, *Int. J. Inorg. Mater.* **2,** 217 (2000).
18. A. Choudhury, S. Natarajan, and C. N. R. Rao, *Chem. Commun.* 1305 (1999).
19. G. M. Sheldrick, *SADABS Siemens Area Detector Absorption Correction Program*; University of Gottingen: Gottingen, Germany 1994.
20. G. M. Sheldrick, "SHELXS-86, A Program for the Solution of Crystal Structures." University of Göttingen, Göttingen, Germany, 1986.
21. H. D. Flack, *Acta Crystallogr. A* **39,** 876 (1983).
22. G. M. Sheldrick, "SHELXTL-PLUS Program for Crystal Structure Solution and Refinement." University of Göttingen, Göttingen, Germany, 1993.
23. I. D. Brown, and D. Aldermatt, *Acta Crystallogr. B.* **41,** 244 (1984).
24. J. B. Goodenough, "Magnetism and the Chemical Bond." Interscience, New York, 1963.
25. S. Neeraj, S. Natarajan, and C. N. R. Rao, *Angew. Chem. Int. Ed.* **38,** 3480 (1999).
26. C. N. R. Rao, S. Natarajan, and S. Neeraj, *J. Am. Chem. Soc.* **122,** 2810 (2000).
27. S. Natarajan, J.-C. P. Gabriel, and A. K. Cheetham, *Chem. Commun.* 1415 (1996).